Korean J. Chem. Eng., 33(2), 465-472 (2016)
DOI: 10.1007/s11814-015-0159-y

pISSN: 0256-1115
eISSN: 1975-7220

Catalytic application of metallic iron from the dyeing sludge ash for benzene steam reforming reaction in tar emitted from biomass gasification

Sung-Bang Nam*, Yeong-Su Park*, Yong-Sik Yun*, Jae-Hoi Gu*, Ho-Jin Sung*,†, and Masayuki Horio**

*Plant Engineering Center, Institute for Advanced Engineering,
633-2, Goan, Baegam, Cheoin, Yongin, Kyeonggi 449-863, Korea
**Department of Chemical Engineering, Graduate School of Bio-Applications and Systems Engineering,
Tokyo University of Agriculture and Technology, 24-16, Naka-cho 2, Koganei-shi, Tokyo 184-8588, Japan
(*Received 30 December 2014 • accepted 21 July 2015*)

Abstract−Because it is the most promising method for reforming tar in a gasification system, a catalytic steam reforming reaction of tar using a dyeing sludge ash catalyst that contains mostly iron oxide has been modeled using benzene to investigate whether a steam reforming catalyst produced from waste is viable. The catalytic activity of the ash catalyst is similar to that of the commercially available iron-chrome-based catalyst for the same equivalent total amount of Fe_2O_3. The activity over the ash catalyst has been examined in terms of the weight hour space velocity (WHSV) and the reaction temperature to develop a model for the reaction kinetics. Using a power law model, the reaction order coefficients of the benzene and steam were estimated to be 0.43 and 0, respectively. The activation energy required for the ash catalyst was approximately 187.6 kJ mol^{-1}. In addition, the reductive properties of the iron oxide in the ash catalyst were also examined via XRD and H_2-TPR analyses.

Keywords: Biomass Gasification, Steam Reforming, Catalytic Tar Reduction, Iron Oxide Catalyst, Benzene

INTRODUCTION

Biomass has received significant and increasing attention as a renewable energy resource, considering the gradual depletion of fossil fuel resources and the worldwide concern on emission of greenhouse gases [1-3]. Studies of gasification, which is a biomass conversion process, have focused on the production of gases rich in CO and H_2, to generate electricity via gas turbines or to produce methanol or such chemical products through catalytic reactions [4]. However, gaseous tar formation is a primary explanation for inefficient gasification processes and the inhibition of downstream process through pipe blockages [5]. These issues increase the cost of this process. The tar produced from the biomass gasification is an undesirable side-product composed of various condensable materials, including polycyclic aromatic hydrocarbons. Similar studies have indicated that high amounts of benzene are present alongside the aromatic hydrocarbons typically found in biomass tar [6]. In addition, benzene exhibits a low coking rate on the catalyst surface owing to its weaker strength of adsorption than that of the other aromatic compounds [7,8]. Thus, benzene has been considered as one of the representative tar species in the present on the preliminary catalyst evaluation.

To remove the tar component from the syngas, catalytic steam reforming has been employed during gasification processes [6,9-12]. The CO and H_2 gases generated by catalytically cracking tar via steam reforming improve the efficiency of biomass gasification processes. Coke formation can be prevented on the catalyst surface by selecting the appropriate steam to carbon ratio and reaction temperature.

Nickel-based catalysts are highly active for tar removal and the reduction of NH_3 which are easily transformed to NOx on gas turbine fired gasification product gas [10]. Although they attain the highest tar-removal efficiencies, the deactivation of nickel-based catalysts via sintering at 650-900 °C poses a significant technical barrier [11]. In addition, nickel-based catalysts are rarely used in fluidized gasifiers due to the particle attribution phenomenon on the gasifier and their rapid deactivation through carbon formation [10].

However, the iron oxide catalysts commonly used for water-gas shift reactions might be used as catalysts for steam reforming of tar due to their superior thermal stability [5,13-15]. Uddin et al. explained that iron oxide catalysts are appropriate for decomposing tar because they are more economical and less harmful than Ni-based catalysts [15]. Reports have also suggested that the role of metallic iron constituent is catalytically important in the active sites for tar destruction during catalytic reforming reactions [16]. Nordgreen et al. reported that the tar content in the syngas during the biomass gasification was decreased when using metallic iron as a tar-depleting catalyst in a fluidized gasifier [17]. Furthermore, the initial activity of a naphthalene steam reforming reaction increased to 90% when using a 70 wt% Fe-Al catalyst at 850 °C [6]. In addition, the mechanism for steam reforming tar over iron oxide is a cyclical process with three steps: (1) the reduction of the Fe_2O_3 to FeO through the syngas from gasification reactions containing H_2 and CO, (2) the transformation of Fe_3O_4 by supplying steam into the gasifier and (3) the destruction of tar through steam reform-

†To whom correspondence should be addressed.
E-mail: hjsung@iae.re.kr

ing over Fe_3O_4.

Eighty million tons of dyeing sludge is generated annually that cannot be buried in landfills or dumped at sea. However, it can be used for reducing the tar emitted during biomass gasification by continuously supplying the gasifier with iron oxide; conventional biomass gasification systems require an extra reactor to charge noble metal catalysts [18-20]. In view of this, the deactivation of iron oxide by sintering or coking is not a major problem in fluidized bed gasification systems using dyeing sludge ash. In addition, the iron oxide in the bottom ash emitted from the gasifier also can be used to catalyze the destruction of tar in a separate reforming reactor. However, no systematic studies have been performed using the iron oxide in biomass waste of the fluidized bed gasifiers or on catalytic steam reforming of tar with bottom ash after gasifying dyeing sludge.

Therefore, the present study investigated the suitability of an ash catalyst, which is composed primarily of iron oxide, for decomposing tar compared with a catalytic steam reforming reaction on a commercially available iron-based catalyst. This paper presents the catalytic activity of dyeing sludge ash and the modelled reaction kinetics of a steam reforming reaction with benzene for various space velocity levels.

EXPERIMENTAL

1. Catalyst Preparation

A dyeing sludge ash-based catalyst (22 wt% Fe_2O_3) was prepared at 900 °C for 10 h in a muffle furnace to eliminate its combustible components with a theoretical air ratio of 2. In addition, a commercially available iron-chrome-based catalyst was employed to examine the activity of a commercial catalyst (88 wt% Fe_2O_3) compared to the dyeing sludge-based ash catalyst.

2. Catalyst Characterization

2-1. XRF (X-ray Fluorescence) Analysis

To determine the Fe content of the ash catalyst, an X-ray fluorescence spectroscopy (XRF) analysis was employed (ZSX Primus II, Rigaku Co.). Crushed samples using boric acid as flux were prepared to minimize the matrix effects. The XRF was equipped with an X-ray tube, an Rh anode and the corresponding filters. In addition, the XRF data were generated using a validated analytical program (UniQuantV4.51 Omega Data Systems).

2-2. BET (Brunauer-Emmett-Teller) Analysis

The BET (Autosorb-1 apparatus, Quantachrome Co.) surface area was calculated based on the N_2 adsorption data obtained using liquid nitrogen at −196 °C. Before the measurements, approximately 0.1 g of a uniformly crushed catalyst sample was pretreated for 6 h under vacuum at 200 °C.

2-3. TPR (Temperature Programmed Reduction) Analysis

To quantify the amount of reducible iron on the ash-based catalyst, an H_2-TPR study was performed using 0.5 g of the catalysts heated at 10 °C/min under a hydrogen atmosphere (5% H_2/Ar) flowing at 30 ml/min (Autochem II 2920, Micromeritics Co.). The iron-chromium- and ash-based catalysts were pretreated before each TPR experiment by using the following procedure: 5% H_2/Ar at 450 °C for 1 h and 5% O_2/Ar at 200 °C for 2 h. A thermal conductivity detector (TCD; Autochem II 2920, Micromeritics Co.) was used to measure the amount of H_2 consumed during the reduction of the metal oxide on the catalyst surface.

2-4. XRD (X-ray Diffraction) Analysis

The powder X-ray diffraction (XRD) patterns of the ash catalyst were obtained with a Rigaku D/max-2500V/PC to investigate the degree of reduction of Fe_2O_3 into Fe_3O_4 by H_2. The incident X-rays were monochromatized to a wavelength of 1.5406 Å with Cu-Kα radiation. The diffraction patterns from 2θ=0-90° were examined at 4.0°/min, while the diffractometer was operated at 40 kV and 200 mA.

3. Catalytic Activity Test

3-1. Components of Tar

Gas chromatography-mass spectrometry (GC/MS) analysis was performed to identify the tar components (Shimadzu 2010 plus, Shimadzu Co.). The GC/MS operating condition was 70 eV ionization potential with the MS interface at 250 °C. The injection port was maintained at 200 °C and the sample was injected in splitless mode. The tar was collected from the bubble fluidized bed type of gasifier (BFBG), which was operated in air under steam atmosphere to keep 0.3 of ER at the reaction temperature of 800 °C using rice husk mixed with dyeing sludge.

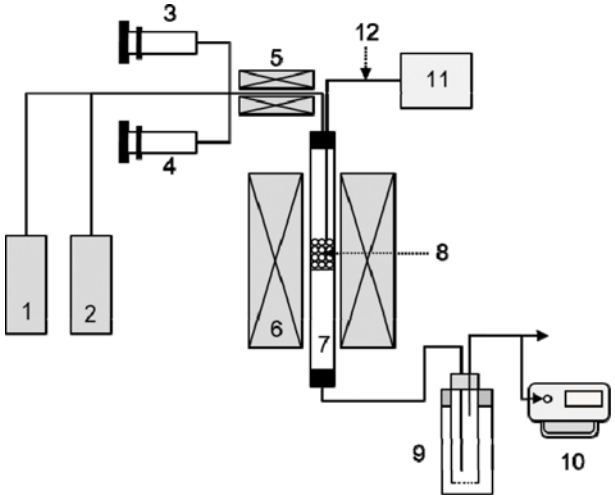

Fig. 1. Schematic flow diagram of catalytic steam reforming reaction system for benzene.

1. H_2	7. Stainless steel reactor
2. N_2	8. Catalyst
3. Syringe pump - Benzene	9. Condenser
4. Syringe pump - Steam	10. Gas chromatography
5. Pre-heater	11. Temperature controller
6. Electric heater	12. Thermocouple

Table 1. Hydrocarbon composition of the biomass gasification tar

HC species	Benzene	Toluene	Naphthalene	Styrene	Acenaphthylene
Concentration (ppm)	175	85	194	63	57

Table 2. Chemical composition of the ash catalyst determined through XRF analysis before and after the experiments

Catalyst	Chemical composition (wt%)						
	Fe	Si	Ca	Al	K	Ti	Mg
Fresh catalyst	27.54	19.23	18.16	9.429	4.093	2.046	1.710
Used catalyst A	27.48	17.97	16.21	8.096	5.262	1.326	1.7033
Used catalyst B	29.16	15.20	18.48	7.302	3.883	2.281	1.7474
Used catalyst C	28.18	16.83	19.43	7.690	4.156	2.156	1.7073
Used catalyst D	26.50	16.20	18.98	7.432	4.081	2.031	1.7649
Used catalyst E	26.52	15.83	19.49	7.510	4.160	2.162	1.7536

Table 3. Textural properties of the ash catalyst determined through BET analysis

Sample	BET specific surface area (m^2/g)	Pore volume (cm^3/g)	Pore size (nm)	Particle size (nm)
Dyeing ash catalyst	8.957	0.03398	151.7	6,692
Commercial catalyst	158.3	0.1927	48.69	378

GC/MS analysis revealed that naphthalene, benzene and toluene are the major components of the resultant tar, as listed in Table 1. These aromatic components presented the range of the structures between 1 and 4. In the present study, the benzene was introduced into the reactor system of Fig. 1 as one of the major components in tar to compare the catalyst activity of tar steam reforming reaction.

3-2. Reaction Condition of Activity Test

The steady-state activity was examined over 3 g of powdered ash catalyst (500) in a packed-bed stainless steel reactor while varying the weight hourly space velocity (WHSV) from 0.15-0.70 h^{-1} and using a steam-to-carbon molar ratio (S/C ratio) of 2, as depicted in Fig. 1. The WHSV and S/C ratio were calculated as follows [21]:

$$\text{WHSV } (h^{-1}) = \frac{60 \times G}{W_{cat}} \quad (1)$$

$$S/C = \frac{2}{3} \times \frac{F_{st} \times \frac{18}{22.4}}{G \times c_p} \quad (2)$$

where F_{st}, G, c_p and W_{cat} designate steam flow rate (L/min), sample flow rate (g-sample/min), carbon weight ratio (−) in the sample feedstock, and the weight of charged catalyst in the reactor (g), respectively. The benzene conversion was simply measured as the ratio of the carbon present in benzene converted to carbon monoxide and carbon dioxide by the following relationship [10]:

$$\text{Conversion of carbon (\%)} = \frac{\text{Carbon mole for CO} + \text{Carbon mole for } CO_2}{\text{Carbon mole for } C_6H_6} \times 100 \quad (3)$$

The feed gas stream containing the liquid steam and benzene phase was added using syringe pumps, and the N_2 making up the balance was added through a mass flow controller. The concentrations of H_2, CH_4, C_3H_6, CO, CO_2 and N_2 gases were analyzed by gas chromatograph (GC) equipped with a TCD (model 3000 micro GC, Inficon Co.). The ash catalysts were precalcined before the experiments under the following reductive condition: 8% H_2 with Ar making up the balance at 500 °C for 1 h. In addition, every experiment was monitored over 2 h.

RESULTS AND DISCUSSION

1. Ash Catalyst Properties

The metallic content of the fresh and used ash catalysts was examined by XRF, as detailed in Table 2. The major components of the dyeing ash catalyst are Fe, Si and Ca with concentrations of 27 wt%, 19 wt% and 18 wt%, respectively. Because it is the active site for steam reforming, the Fe content of the catalysts is strongly related to their catalytic activity. The used catalysts were selected at WHSV from 0.70 to 0.15 h^{-1} at 900 °C and at temperatures from 800 to 900 °C at a WHSV of 0.15 h^{-1}. Similar metallic content was observed for the used and fresh catalysts regardless of the reaction conditions.

The textural properties of the ash and commercially available catalyst characterized via BET analysis are listed in Table 3. The BET surface area (8.957 m^2/g) of the ash catalyst may be closely related to the low dispersion of active sites, even though it contained the most Fe species (27 wt%). The low dispersion might occur because no porous materials are available to support the metal particle on the surface of the ash-based catalyst from the dyeing sludge, while the commercial catalyst showed 158.3 m^2/g of BET surface area. In addition, the particle size of ash was 6,692 nm, which is 20 times higher than that of commercial catalyst (378 nm). In view of this, the dyeing sludge ash may not have catalyst structure compared to commercial catalyst. However, the dyeing sludge ash, which is formed above 900 °C, could be superior thermal durability as commercial catalysts.

2. Comparison of Catalytic Activity

The catalytic activity during the steam reforming reactions of benzene was assessed over the ash-based and commercial iron-chromium-based catalysts, as shown in Fig. 2. These experiments were performed at a WHSV of 0.15 h^{-1}, a retention time of 0.3 s and different reaction temperature with an equivalent amount of Fe_2O_3 loaded onto catalyst. Recently, the gasification temperature for biomass has increased to 850 °C from 800 °C primarily caused by the cracking conditions of polyaromatic hydrocarbons and the hydrogen yield [1,22]. Therefore, temperatures of 800, 850 and 900 °C

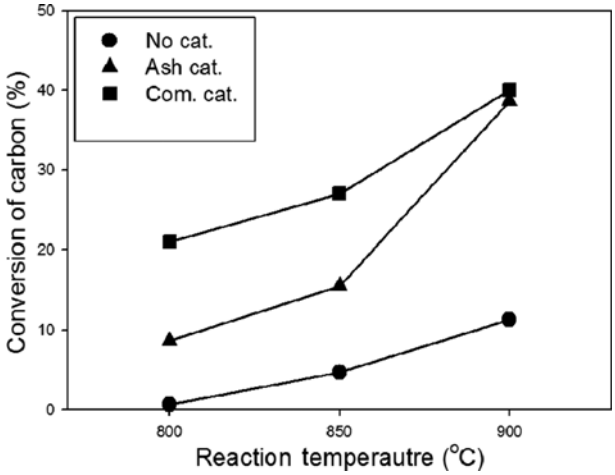

Fig. 2. Comparison of catalytic activity over no catalyst, ash catalyst and commercial catalyst for steam reforming reaction of benzene, reaction condition: WHSV=0.15 h^{-1}, RT=0.30 s and S/C=2.

Table 4. Chemical composition of the iron-chrome-based commercial catalyst

Composition (wt%)	Fe_2O_3	Cr_2O_3	CuO	S	Cl
	88	8.1	2.5	0.009	0.003

were employed in the present study. Similar reaction activity test was also performed under homogeneous gas-phase conditions to evaluate the enhancement of the reaction provided by the catalysts.

The commercially available catalyst including 88 wt% of Fe_2O_3 was more reactive than the ash catalyst at temperatures from 800 to 850 °C, as shown in Table 4. The differences in the carbon conversion over the commercial and ash catalysts were 12% and 13% at 800 °C and 850 °C, respectively. However, the maximum carbon conversions over both catalysts were quite similar (40% conversion) because the Cr and Cu used as promoters improved the catalytic activity of the commercially available catalyst at lower reaction temperatures [23]. However the activated Fe played a more critical role in the active sites for steam reforming of benzene at 900 °C. The carbon conversion increased in the presence of the catalyst over the entire temperature range in view of the fact that 11% carbon conversion was observed at 900 °C under homogeneous reaction conditions. Therefore, the destruction of tar over the ash catalyst could reduce the operational costs by replacing the commercial catalyst and allowing a continuous feed into the gasifier by acting as a bed medium.

Note that the various parallel reactions can take place consecutively during the gasification due to the complexity of gas components from the gasifier [10]. The conventional reactions by the steam are including steam reforming reactions (Eq. (4) and Eq. (5)) and water-gas shift reaction (Eq. (6)) as follows:

$$C_6H_6+6H_2O\rightarrow 6CO+9H_2 \quad (4)$$

$$C_6H_6+12H_2O\rightarrow 6CO_2+15H_2 \quad (5)$$

$$CO+H_2O\rightarrow CO_2+H_2 \quad (6)$$

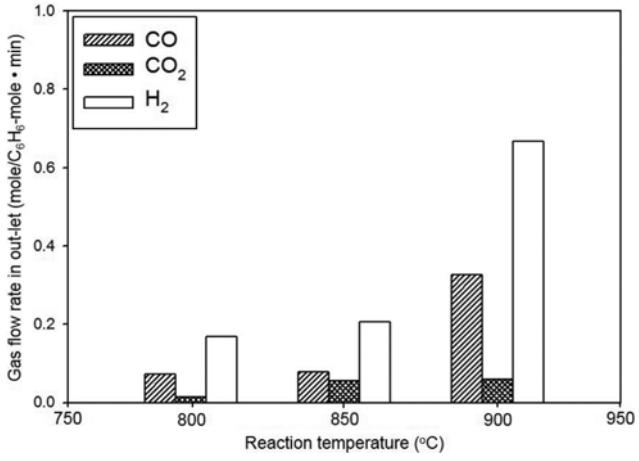

Fig. 3. Comparison of flow rate ratio of products from steam reforming benzene over the ash catalyst under the following reaction conditions: WHSV=0.15 h^{-1}, RT=0.30 s and S/C=2.

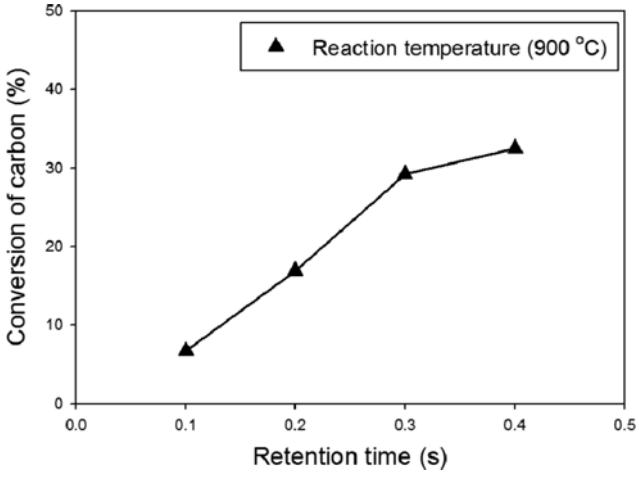

Fig. 4. Activity over ash catalyst with respect to retention time, reaction condition: WHSV=0.5 h^{-1}, reaction temperature=900 °C and S/C=2.

To determine the catalytic reaction path occurring on the ash catalyst, the flow rate ratio (mole/benzene mole·min) of gas product was compared with respect to the reaction temperature, as depicted in Fig. 3. The H_2 was the most abundantly produced among the gas products at all reaction temperatures. Note that the CO productivity was enhanced with the increase of reaction temperature, while a moderate amount of CO_2 was produced above the 850 °C. This could be related to the fact that the steam reforming reaction is more thermodynamically favorable than the water-gas shift reaction with the increasing reaction temperature [24,25]. In addition, the CO_2 was produced stoichiometrically by the water-gas shift reaction governed by the moles of H_2 produced. For example at 900 °C, the production yield of H_2 for steam reforming reaction (Eq. (4)) was 91%, while the only 9% of H_2 yield was observed by the water-gas shift reaction (Eq. (6)).

3. Effect of Retention Time

To understand the limitations of external diffusion, the catalytic activity was examined over the ash-based catalyst as a function of

the retention time from 0.1 to 0.4 s at a WHSV of 0.5 h^{-1} and a reaction temperature of 900 °C, as shown in Fig. 4. The retention time was varied by changing the total flow rate except but not the benzene and steam flow rates.

An approximately five-fold increase in the carbon conversion was observed after increasing the retention time from 0.1 to 0.3 s, while the 2% carbon conversion was enhanced by increasing the retention time from 0.3 to 0.4 s. The influence of external diffusion on the catalytic activity for steam reforming of benzene over the ash-based catalyst was observed to be optimized at retention time longer than 0.3 s.

4. Effect of the Weight Hourly Space Velocity (WHSV)

To evaluate the kinetic parameters of the steam reforming reaction over the ash-based catalyst, the activity of the catalyst was tested relative to the weight hourly space velocity (WHSV). The WHSV affects catalytic activity via the contact time of the reactants on the catalyst surface [26]. The contact time is defined as follows:

$$\text{Contact time} = \frac{M \cdot W \cdot C_6H_6}{WHSV} \quad (7)$$

Therefore, WHSV was controlled by the benzene flow rate with 3 g of the ash catalyst charged into the reactor at various temperatures (800, 850 and 900 °C), a retention time of 0.3 s and a steam to carbon ratio of 2.

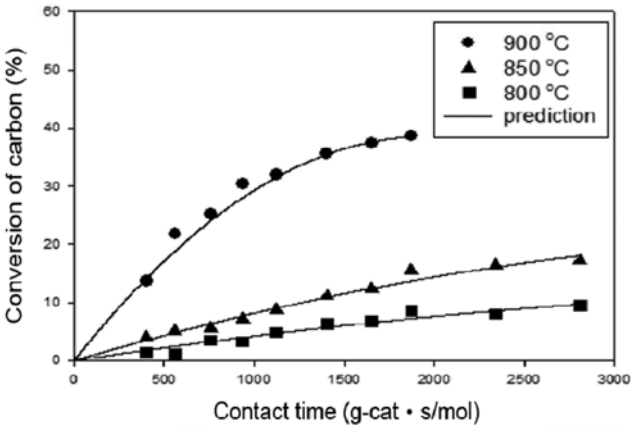

Fig. 5. Activity over the ash catalyst relative to the WHSV under the following reaction conditions: RT=0.30 s, reaction temperature=800, 850 and 900 °C and S/C=2.

Table 5. Comparison of the observed reaction rates with the predicted reaction rates from least square method

Reaction temperature (°C)	Carbon conversion (%)	Partial pressure (kpa)		Observed reaction rate (mol/kg-cat·s)	Estimated reaction rate (mol/kg-cat·s)
		Benzene	Steam		
800	1.30	3.22	38.59	4.32×10^{-2}	5.56×10^{-2}
	0.90	2.31	27.67	4.18×10^{-2}	4.84×10^{-2}
	3.50	1.71	20.53	4.01×10^{-2}	4.20×10^{-2}
	1.80	1.39	16.67	3.86×10^{-2}	3.88×10^{-2}
	2.80	1.16	13.90	3.69×10^{-2}	3.58×10^{-2}
	6.30	0.93	11.13	3.45×10^{-2}	3.20×10^{-2}
	6.80	0.79	9.47	3.24×10^{-2}	2.98×10^{-2}
	8.60	0.70	8.36	3.05×10^{-2}	2.80×10^{-2}
	8.00	0.56	6.69	2.65×10^{-2}	2.56×10^{-2}
	9.50	0.46	5.58	2.25×10^{-2}	2.35×10^{-2}
850	3.00	3.36	40.36	8.33×10^{-2}	1.04×10^{-1}
	5.10	2.41	28.95	8.02×10^{-2}	8.91×10^{-2}
	5.60	1.79	21.48	7.65×10^{-2}	7.83×10^{-2}
	6.60	1.45	17.44	7.31×10^{-2}	7.12×10^{-2}
	8.70	1.21	14.55	6.95×10^{-2}	6.52×10^{-2}
	11.10	0.97	11.65	6.42×10^{-2}	5.87×10^{-2}
	12.30	0.83	9.91	5.95×10^{-2}	5.46×10^{-2}
	15.50	0.73	8.75	5.53×10^{-2}	5.10×10^{-2}
	16.40	0.58	7.00	4.64×10^{-2}	4.59×10^{-2}
	17.20	0.49	5.84	3.75×10^{-2}	4.25×10^{-2}
900	13.70	3.58	42.97	2.53×10^{-1}	3.26×10^{-1}
	21.80	2.58	30.96	2.39×10^{-1}	2.72×10^{-1}
	25.10	1.92	23.04	2.22×10^{-1}	2.33×10^{-1}
	30.30	1.56	18.74	2.07×10^{-1}	2.09×10^{-1}
	31.90	1.30	15.65	1.91×10^{-1}	1.93×10^{-1}
	35.50	1.05	12.55	1.66×10^{-1}	1.71×10^{-1}
	37.30	0.89	10.68	1.45×10^{-1}	1.58×10^{-1}
	38.60	0.79	9.43	1.26×10^{-1}	1.49×10^{-1}

As shown in Fig. 5, a positive trend was observed in terms of carbon conversion when decreasing the WHSV from 0.70 to 0.15 h^{-1} regardless of the reaction temperature. In addition, the catalytic activity of the ash catalyst at 900 °C was higher than that at 800 and 850 °C relative to the contact time. The maximum conversion of carbon (40%) was obtained at a WHSV of 0.2 h^{-1} and a reaction temperature of 900 °C.

5. Kinetic Studies of the Catalytic Steam Reforming Reaction over Ash Catalyst

The reaction kinetics for steam reforming of benzene over the ash-based catalyst was comprehensively investigated via a differential analysis [21]. The equation for the steam reforming reaction can be expressed in terms of the benzene concentration for zeroth-order in water [6]. Garcia et al. reported that the reaction rate for steam reforming of benzene over dolomite was independent of the steam partial pressure, considering the effect of the steam to carbon ratio [27]. The kinetic data were obtained by changing the partial pressure of the reactants at a constant total pressure (101.325 kPa) while maintaining steam to carbon ratio of 2 at reaction temperatures of 800, 850 and 900 °C. The chemical kinetics of hydrocarbon steam reforming reactions was proposed using the empirical power law model for the reaction rate and partial pressures as follows [27-29]:

$$r = kP_{C_xH_y}^{a} P_{H_2O}^{b} \quad (8)$$

Although an extensive literature survey was made, the reaction kinetics on the catalytic steam reforming reaction of tar over the ash catalyst has rarely been considered. Therefore, it was desired to generate comprehensive kinetic data as a technical guide to decrease tar emissions during gasification process, especially related to the use of ash with improved catalytic performance. The reaction constant and order of the power law model for steam reforming reaction of benzene were estimated using a least squares method. From above results, the estimated reaction rates from least square method were compared to observed reaction rate as listed in Table 5. In addition, the activation energy (E) and pre-exponential factor (A) of the rate constant, which are temperature dependent, were determined using the Arrhenius equation. The estimated values including the reaction orders, activation energy and pre-exponential factor are listed in Table 6. The rate equation for steam reforming of benzene over the ash catalyst was obtained as follows:

$$r = 3.815 \times 10^{7} e^{-186.7} P_{C_6H_6}^{0.43} P_{H_2O}^{0} \quad (9)$$

The observed and predicted reaction rates thus calculated for the steam reforming reaction with benzene are compared in Fig. 6. The observed reaction rates agreed reasonably well with the predicted ones, while the observed difference was quite insignificant below 850 °C.

Table 6. Estimated reaction constants including the activation energy, frequency factor and reaction order for benzene and steam

Parameter	Estimated value
A (mol g-cat^{-1} s^{-1} kPa^{-2})	3.815×10^{7}
E (kJ mol^{-1})	186.7
Reaction order of benzene	0.43
Reaction order of steam	0

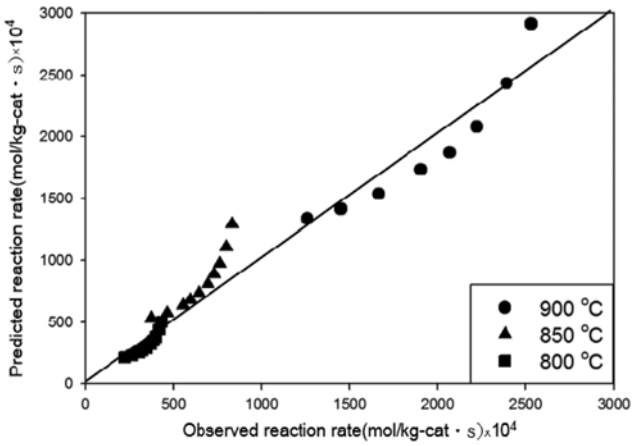

Fig. 6. Comparison of the predicted reaction rates with the observed rates for steam reforming benzene.

6. XRD Study

XRD analysis was conducted to examine the structural changes in the iron oxide from Fe_2O_3 to Fe_3O_4 on the ash catalyst during a reduction by H_2. In preparation for XRD experiments, samples were reduced under H_2 at 500 °C for 1-5 min. The X-ray diffraction peaks were compared with those of the fresh ash catalyst prior to the H_2 treatment, as shown in Fig. 7. Note that the relative intensity of the X-ray diffraction patterns is maintained at an identical scale.

The X-ray diffraction patterns for Fe_2O_3 were obtained on the ash catalyst up to 1 min (Fig. 7(a) and (b)). After 2 min reduction of the ash catalyst under H_2, a peak for Fe_3O_4 was observed which was attributed to a partial transformation of hematite (Fe_2O_3 with

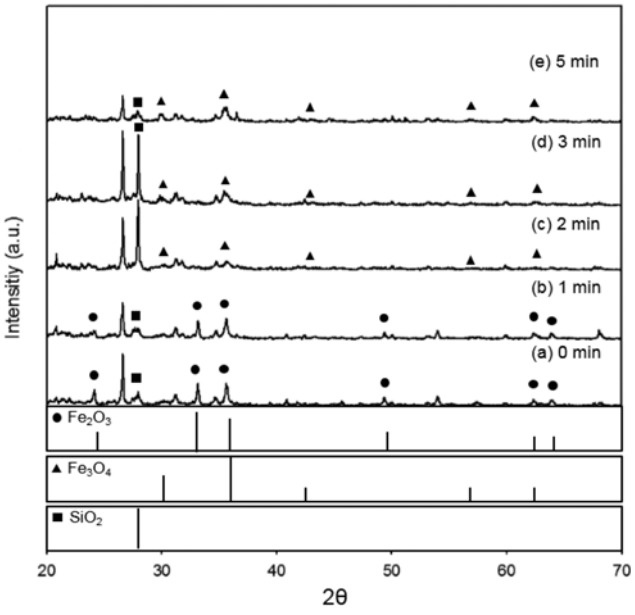

Fig. 7. XRD patterns of the ash catalyst without the H_2 treatment (a) and relative to the reduction time at 500 °C from 1 to 5 min ((b)-(e)), respectively.

peaks at 33° and 36°, JCPDS card 33-0664) into magnetite (Fe_3O_4 with peaks at 30° and 36°, JCPDS card 19-0629), as shown in Fig. 7(c). As the reduction time increased to 3 min, only the intense peaks corresponding to Fe_3O_4 were observed (Fig. 7(d)). In Fig. 7(e), the intensity of the Fe_3O_4 diffraction peak asymptotically approached a plateau for samples H_2 reduced for 3 to 5 min. Similar XRD patterns were previously reported on the effect of the reduction time on structural change of α-Fe_2O_3 [30]. Lee et al. also observed that the magnetite patterns were clearly presented with increase of reduction time by the partial transformation from hematite. However, the continuous transient reduction behavior on the ash catalyst was not clearly substantiated over a wide range of temperature based on XRD analyses.

7. H_2-TPR Study

Because it is an active site for decomposing tar, the iron species on the surface of the iron oxide catalyst can be obtained after reducing Fe_2O_3 [14]. Therefore, an H_2-TPR analysis was conducted with the ash- and commercially available iron-chrome-based catalysts for comparison with the reference peak (iron oxide) to assess the reduction behavior of the ash catalyst.

Fig. 8 shows the H_2-TPR profiles of the ash- and commercially available iron-chrome-based catalysts. A major peak at approximately 350 °C was observed for both catalysts at all temperatures, and the intensity of the peak was nine-fold higher for the commercial catalyst relative to the ash-based catalyst. This discrepancy may be associated with the difference in the Fe_2O_3 content, which was 22 wt% for the ash-based catalyst and 88 wt% for the commercial catalyst. In particular, a gradual increase was observed in the amount of H_2 consumed by iron oxide above 500 °C for both catalysts. Munteanu et al. reported that the peak at 350 °C could be attributed to the reduction of Fe_2O_3 to Fe_3O_4, and the high temperature peak at about 630 °C could be related to the reduction from Fe_3O_4 to FeO [31]. Therefore, the metallic iron connected to Fe_3O_4 and FeO is an active species during the benzene steam reforming reaction over both the ash- and commercial iron-chromium-based catalysts. Polychronopoulou et al. reported that the dissociative adsorption of phenol as biomass tar on the iron oxide surface was primarily caused by high ratio of Fe^{2+}/Fe^{3+} in the Fe_2O_3 and FeO [32]. In addition, the metallic iron species on the surface of the iron-based catalysts decomposed tar, which was synergistically related to the bulk Fe_3O_4 of the iron-based catalysts [15]. Therefore, reducing the Fe_2O_3 is necessary step for adsorbing the tar on the ash-based catalyst.

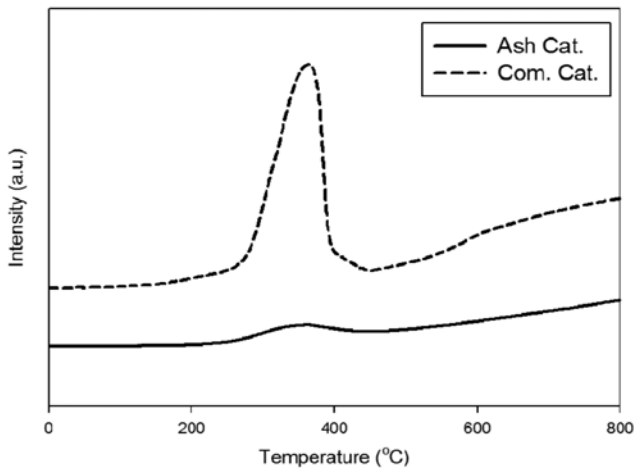

Fig. 8. H_2-TPR profiles of the ash catalyst and commercial iron-chrome based catalyst.

CONCLUSION

To determine its suitability for decomposing tar over the dyeing sludge ash, a catalytic steam reforming reaction with benzene as one of typical tar components was investigated over an ash catalyst that contains 22 wt% Fe_2O_3. From the XRF analysis, the uniform Fe content of the ash catalyst was determined regardless of the reaction conditions. Below 850 °C, the initial carbon conversion over the ash catalyst is lower than that of the commercial iron-chrome-based catalyst due to the absence of a promoter, such as Cr and Cu, on the ash catalyst. However, a similar reaction activity (carbon conversion of 40%) was observed over both catalysts based on an equivalent amount of Fe_2O_3. In addition, external diffusion does not contribute to the catalytic activity over the ash catalyst during benzene steam reforming over a 0.3-s retention time. Therefore, the effect of the WHSV on the activity over the ash catalyst has been investigated over a retention time of 0.3 s at various temperatures. As the WHSV decreases, the activity over ash catalyst has been improved due to the increased contact time between the catalyst surface and reactant regardless of the temperature. The results indicate that the reaction rate determined through a power law model was a good prediction of the observed reaction rate. To understand the reduction properties of the Fe_2O_3 in the ash catalyst, XRD and H_2-TPR analyses were conducted. The changes in the iron oxide structure on the ash catalyst produced from the dyeing sludge were monitored through XRD analysis. The H_2-TPR experiments revealed that the metallic iron of the Fe_3O_4 and FeO from the reduction of Fe_2O_3 over the ash catalyst is related to the active sites when steam reforming benzene.

The dyeing sludge ash catalyst presented low catalyst activity (40% of maximum conversion) compared to the reported literatures using the Ni-based catalyst. Unlike the commercial catalysts, the fresh of ash catalyst can be continuously fed into the gasifier as gasification medium in fluidizing gasifier and secondary reactor as tar reforming catalyst. Consequently, destroying tar through a process using an ash catalyst is expected to reduce the operational cost and to provide a useful guideline for optimizing the process.

ACKNOWLEDGEMENTS

This subject is supported by Korea Ministry of Environment (MOE) as "Waste-to-Energy Technology Development Project" (No. 2013001530001).

REFERENCES

1. L. Devi, K. J. Ptasinski, F. J. J. G. Janssen, S. V. B. van Paasen, P. C. A. Bergman and J. H. A. Kiel, *Ren. Eng.*, **30**, 565 (2005).
2. P. Mckendry, *Bio. Technol.*, **83**, 55 (2002).
3. U. W. E. A. Schneider and B. A. McCarl, *Environ. Res. Econ.*, **24**,

291 (2003).
4. J. Han and H. Kim, *Renew. Sustain. Energy Rev.*, **12**, 397 (2008).
5. H. Noichi, A. Uddin and E. Sasaoka, *Fuel Process Technol.*, **91**, 1609 (2010).
6. R. Coll, J. Salvado, X. Farriol and D. Montane, *Fuel Process Technol.*, **74**, 19 (2001).
7. L. Xu, J. Liu, Q. Wang, S. Liu, W. Xin and Y. Xu, *Appl. Catal.*, **258**, 47 (2004).
8. M. Nagao and Y. Suda, *Langmuir*, **5**, 42 (1989).
9. T. A. Milne, R. J. Evans and N. Abatzoglou, *Technical Report*; NREL: USA, NREL/TP-570-25357, November (1998).
10. D. Swierczynski, S. Libs, C. Courson and A. Kiennemann, *Appl. Catal. B: Environ.*, **74**, 211 (2007).
11. R. Zhang, Y. Wang and R. C. Brown, *Eng. Convers. Manage.*, **48**, 68 (2007).
12. K. Polychronopoulou, A. Bakandritsos, V. Tzitzios, J. L. G. Fierro and A. M. Efstathiou, *J. Catal.*, **241**, 132 (2006).
13. M. A. Edwards, D. M. Whittle, C. Rhodes, A. M. Ward, D. Rohan, M. D. Shannon, G. J. Hutchings and C. J. Kiely, *Phys. Chem. Chem. Phys.*, **4**, 3902 (2002).
14. P. Kumar and R. Idem, *Eng. Fuels*, **21**, 522 (2007).
15. M. D. A. Uddin, H. Tsuda, S. Wu and E. Sasaoka, *Fuel*, **87**, 451 (2008).
16. D. Ross. R. Noda, M. Horio, A. Kosminski, P. Ashman and P. Mullinger, *Fuel*, **86**, 1417 (2007).
17. T. Nordgreen, T. Liliedahl and K. Sjöström, *Fuel*, **85**, 689 (2006).
18. K. Tomishige, T. Miyazawa, M. Asadullah, S. Ito and K. Kunimori, *Green. Chem.*, **5**, 399 (2003).
19. K. Tomishige, M. Asadullah and K. Kunimori, *Catal. Today*, **89**, 389 (2004).
20. D. Sutton, B. Kelleher and J. R. H. Ross, *Fuel Process Technol.*, **13**, 155 (2001).
21. Y. S. Park, *Ph.D. Dissertation*, Tokyo Institute of Technology, Tokyo, Japan (2012).
22. N. Gao, A. Li, C. Quan and F. Gao, *Int. J. Hydrogen Energy*, **33**, 5430 (2008).
23. L. Ma, B. Gong, T. Tran and M. S. Wainwright, *Catal. Today*, **63**, 499 (2000).
24. K. K. Pant, R. Jain and S. Jain, *Korean J. Chem. Eng.*, **28**, 1859 (2011).
25. P. Kuchonthara, B. Puttasawat, P. Piumsomboon, L. Mekasut and T. Vitidsant, *Korean J. Chem. Eng.*, **29**, 1525 (2012).
26. M. B. Talawar, T. M. Jyothi, P. D. Sawant, T. Raja and B. S. Raw, *Green. Chem.*, **2**, 266 (2000).
27. X. A. Garcia and K. J. Hüttinger, *Erdöl Kohle Erdgas Petrochem.*, **43**, 273 (1990).
28. C. H. Bartholomew, *Appl. Catal. A: Gen.*, **212**, 17 (2001).
29. E. G. Baker, L. K. Mudge and M. D. Brown, *Ind. Eng. Chem. Res.*, **26**, 1335 (1987).
30. G. H. Lee, J. G. Park, Y. M. Sung, K. Y. Chung, W. I. Cho and D. W. Kim, *Nanotechnol.*, **20**, 295205 (2009).
31. G. Munteanu, L. Ilieva and D. Andreeva, *Thermochim. Acta*, **291**, 171 (1997).
32. K. Polychronopoulou, A. Bakandritsos, V. Tzitzios, J. L. G. Fierro and A. M. Efstathiou, *J. Catal.*, **241**, 132 (2006).